

In Vitro Interactions between the P_{II} Proteins and the Nitrogenase Regulatory Enzymes Dinitrogenase Reductase ADP-ribosyltransferase (DraT) and Dinitrogenase Reductase-activating Glycohydrolase (DraG) in *Azospirillum brasilense*^{*[5]}

Received for publication, September 24, 2008, and in revised form, January 8, 2009. Published, JBC Papers in Press, January 8, 2009, DOI 10.1074/jbc.M807378200

Luciano F. Huergo^{†1}, Mike Merrick^{§2}, Rose A. Monteiro[‡], Leda S. Chubatsu[‡], Maria B. R. Steffens[‡], Fábio O. Pedrosa[‡], and Emanuel M. Souza[†]

From the [‡]Department of Biochemistry and Molecular Biology, Universidade Federal do Paraná, CP 19046, 81531-990 Curitiba-PR, Brazil and the [§]Department of Molecular Microbiology, John Innes Centre, Norwich NR4 7UH, United Kingdom

The activity of the nitrogenase enzyme in the diazotroph *Azospirillum brasilense* is reversibly inactivated by ammonium through ADP-ribosylation of the nitrogenase NifH subunit. This process is catalyzed by DraT and is reversed by DraG, and the activities of both enzymes are regulated according to the levels of ammonium through direct interactions with the P_{II} proteins GlnB and GlnZ. We have previously shown that DraG interacts with GlnZ both *in vivo* and *in vitro* and that DraT interacts with GlnB *in vivo*. We have now characterized the influence of P_{II} uridylylation status and the P_{II} effectors (ATP, ADP, and 2-oxoglutarate) on the *in vitro* formation of DraT-GlnB and DraG-GlnZ complexes. We observed that both interactions are maximized when P_{II} proteins are de-uridylylated and when ADP is present. The DraT-GlnB complex formed *in vivo* was purified to homogeneity in the presence of ADP. The stoichiometry of the DraT-GlnB complex was determined by three independent approaches, all of which indicated a 1:1 stoichiometry (DraT monomer:GlnB trimer). Our results suggest that the intracellular fluctuation of the P_{II} ligands ATP, ADP, and 2-oxoglutarate play a key role in the post-translational regulation of nitrogenase activity.

Biological nitrogen fixation is catalyzed by the nitrogenase enzyme and is a very energy-demanding process requiring at least 16 mol of ATP per mol of N₂ reduced. Consequently it is tightly regulated both at the transcriptional and, in some cases, at the post-translational level (1). In some free-living bacteria, nitrogenase is down-regulated at the post-translational level by reversible ADP-ribosylation of the nitrogenase Fe-protein or NifH. This modification is catalyzed by dinitrogenase reductase

ADP-ribosyltransferase (DraT)³ and is reversed by dinitrogenase reductase-activating glycohydrolase (DraG) (2, 3). Nitrogenase inactivation is induced by ammonium in the external medium or by a decrease in the energy charge of the cell, the main component of which is the ATP/ADP ratio (4, 5). In *Azospirillum brasilense*, the latter response occurs upon an anaerobic shift whereas in *Rhodospirillum rubrum* and *Rhodobacter capsulatus* it occurs in response to darkness (2, 3).

The model for DraT and DraG regulation suggests that DraT is inactive and DraG is active before the cell is exposed to a negative stimulus for nitrogenase (3). When ammonium is added to the medium, DraT is transiently activated and DraG is inactivated leading to NifH modification and inactivation. The DraG enzyme is reactivated as the negative stimulus is exhausted, causing NifH re-activation (3). Recently, several features of the ammonium-signaling pathway that control DraT and DraG activities have begun to be understood (6–12). In all cases, regulation of DraT and DraG appears to involve direct interaction between these enzymes and the nitrogen-signaling P_{II} proteins. In *A. brasilense*, which encodes two P_{II} proteins, GlnB and GlnZ (13), a model for this process has recently been proposed (10). Upon an ammonium shock, GlnB interacts with DraT, and this is presumed to trigger DraT activation. GlnZ interacts with both DraG and the ammonium transporter AmtB on the cell membrane. The formation of a ternary complex between AmtB, GlnZ, and DraG efficiently targets DraG to the cell membrane where it is presumed to be catalytically inactive (10, 12).

The P_{II} protein family is very widely distributed, and several features of these proteins have been recently reviewed (14, 15). P_{II} proteins are trimeric proteins that control cellular nitrogen metabolism by direct protein-protein interaction with several enzymes, transcriptional regulators, and transporters. The structures of P_{II} proteins from several organisms have been determined, and they are in general highly conserved. The trimer consists of a core compact barrel with three protruding

* This work was supported in part by CNPq and Fundação Araucária. The costs of publication of this article were defrayed in part by the payment of page charges. This article must therefore be hereby marked "advertisement" in accordance with 18 U.S.C. Section 1734 solely to indicate this fact.

[5] The on-line version of this article (available at <http://www.jbc.org>) contains supplemental Figs. S1–S7 and Table S1.

¹ Supported by a PDJ fellowship from the CNPq-Brazil. To whom correspondence should be addressed. Tel.: 55-41-3361-1657; Fax: 55-41-3366-4398; E-mail: huergo@ufpr.br.

² Received support from the Biotechnology and Biological Sciences Research Council (UK).

³ The abbreviations used are: DraT, dinitrogenase reductase ADP-ribosyltransferase; DraG, dinitrogenase reductase-activating glycohydrolase; 2-OG, 2-oxoglutarate; LDAO, lauryldimethylamine oxide; GS, glutamine synthetase; GOGAT, glutamate synthase.

loops: the T, B, and C loops (16, 17). P_{II} protein activity is regulated through binding of the allosteric effectors ATP, ADP, and 2-oxoglutarate (2-OG). In many cases, these proteins are also regulated by covalent modification of the T-loop. This can involve uridylylation in Gram-negative bacteria (18), adenylation in Gram-positive bacteria (19), and phosphorylation in cyanobacteria (20). The P_{II} proteins from *Escherichia coli* can bind up to three molecules of ATP and 2-OG in a positive synergistic manner (21), the ATP-binding site being located in the lateral clefts between the subunits (17, 22). Co-crystallization of *Methanococcus jannaschii* GlnK with Mg-ATP and 2-OG suggested that Mg-ATP binding to the lateral cleft causes the T-loop to assume a compact conformation that creates a 2-OG-binding site in the T-loop. In this structure, 2-OG is accommodated mainly by hydrogen bond formation with the main chain backbone (23). Recent data from several organisms indicate that the P_{II} ATP-binding site can be occupied by ADP in a competitive manner, suggesting that P_{II} proteins can act as sensors of the energy charge of the cell (12, 23–27).

The *A. brasilense* P_{II} proteins, GlnB and GlnZ, are subject to a cycle of uridylylation/de-uridylylation catalyzed by the bifunctional enzyme GlnD (28, 29). Under nitrogen-limiting conditions GlnB and GlnZ are fully uridylylated, and upon an ammonium shock GlnD promotes their de-uridylylation (28, 30, 31). *In vivo* experiments in *A. brasilense* have shown that the uridylylation cycle of the P_{II} proteins in response to ammonium is synchronized with nitrogenase ADP-ribosylation and hence with changes in DraT and DraG activities (11). Previous results have shown that de-uridylylated GlnZ and GlnB can interact with DraG and DraT, respectively, in *A. brasilense* (10). In this detailed study, we have now characterized the influence of P_{II} uridylylation status and the P_{II} effectors on *in vitro* formation of DraT-GlnB and DraG-GlnZ complexes. We have also determined the stoichiometry of the DraT-GlnB complex.

EXPERIMENTAL PROCEDURES

Protein Analysis—Electrophoresis of proteins was carried out by SDS-PAGE, and gels were Coomassie Blue-stained unless indicated otherwise. Signals on gels were quantified using the Lab Works (UVP) or the ImageQuant (GE Healthcare) software where results are reported in arbitrary units. Protein concentrations were determined by the Bradford assay using bovine serum albumin as a standard. Western blots were carried out as described, using polyclonal rabbit anti-DraT antibody (11). MALDI-TOF analysis was performed as described previously (30).

Protein Purification—The *A. brasilense* GlnB, GlnZ, His-GlnD, HisDraG, and HisDraT proteins were purified as described previously (12, 30, 32). For the purification of the HisDraT-GlnB complex, both proteins were co-expressed in *E. coli* BL21 from the plasmids pLHPETDraT (32) and pLHDK5pII (33) overnight at 20 °C using isopropyl-1-thio- β -D-galactopyranoside 0.3 mM as inducer. The complex was purified using a 1-ml HiTrap-chelating Ni²⁺ column (GE Healthcare) with a non-linear imidazole gradient in Tris-HCl, 50 mM, pH 8, NaCl, 100 mM, MgCl₂, 1 mM, ADP, 0.5 mM, and glycerol 10% (v/v). Imidazole concentrations used were 10, 50, 100, 300, and 500 mM; the HisDraT-GlnB complex eluted at 300 mM.

After elution with imidazole from the HiTrap chelating Ni²⁺ column, HisDraG, HisDraT, and the DraT-GlnB complex were partially precipitated. The samples were centrifuged at 10,000 \times g for 10 min at 4 °C, and only the supernatant was used for further analysis. Proteins were dialyzed to remove imidazole. Typical protein preparations were more than 90% homogeneous judged by densitometry analysis of Coomassie Blue-stained SDS-PAGE gel. Proteins were kept at –80 °C until use.

In Vitro Uridylylation of GlnB and GlnZ—*In vitro* uridylylation of GlnB and GlnZ was performed as described previously (30). The products of the reactions were analyzed by native gel electrophoresis and MALDI-TOF spectrometry as described (30). After the uridylylation reaction, His-GlnD was removed from the system using MagneHis-Ni²⁺ beads (Promega Co, Madison, WI). Fully uridylylated GlnB and GlnZ were dialyzed against 50 mM Tris-HCl, pH 7.5, 0.1 M KCl, 20% glycerol overnight at 4 °C to remove ATP and 2-OG.

Pull-down Assays—*In vitro* complex formation was performed using MagneHis-Ni²⁺ beads according to the manufacturer's instructions (Promega). For HisDraG-GlnZ interaction the reactions were conducted in buffer containing 50 mM Tris-HCl, pH 8, 0.1 M NaCl, 0.05% (w/v) LDAO, 10% glycerol, 20 mM imidazole, and 1 mM MgCl₂ in the presence or absence of effectors (2-OG, ATP, ADP, AMP) as indicated in each experiment. For HisDraT-GlnB interaction, the same buffer was used except that LDAO was substituted by Tween 20 (0.05%, v/v). Ten microliters of beads were equilibrated by two washes with 100 μ l of buffer. Binding reactions were performed in 500 μ l of buffer by adding purified proteins to 0.5 μ M. Protein concentrations were calculated assuming GlnB and GlnZ to be trimers and DraG and DraT to be monomers. After 5 min of incubation at room temperature, the beads were washed three times with 250 μ l of buffer. Elution was performed by incubating the beads either with 20 μ l of buffer containing 0.5 M imidazole for 5 min (when His-DraG was used as bait) or with 30 μ l of SDS-PAGE sample buffer 1 \times and boiled for 5 min (when His-DraT was used as bait). Eluted samples were analyzed in 12.5% SDS-PAGE stained with Coomassie Blue. For complex dissociation assays, the beads were washed with 20 μ l of buffer containing the effectors prior to elution.

Quantitative SDS-PAGE Analysis of the DraT-GlnB Complex—Samples were subjected to SDS-PAGE 12.5% and stained with SYPRO-Ruby (Invitrogen). The intensity of the bands was converted to protein concentration using a calibration curve of both pure His-DraT and GlnB present in the same gel. Each gel was loaded with five different dilutions of the standards GlnB (1.69, 3.37, 6.74, 13.47, and 26.94 pmol of trimer), His-DraT (1.68, 3.35, 6.69, 13.39, and 26.78 pmol of monomer) and the pure DraT-GlnB complex (4, 2, 1, 0.5, and 0.25 μ g). The amount of protein loaded was determined by the Bradford assay. The SYPRO-Ruby signal was recorded using a Biochemi system (UVP) and quantified using the ImageQuant software (GE Healthcare).

Gel Filtration—Gel filtration chromatography was performed on a Superose 12 10/30 GL column using 50 mM Tris-HCl, pH 8.0, 10% (v/v) glycerol, 0.05% (w/v) Tween 20, 100 mM NaCl, 1 mM MgCl₂, 1 mM ADP as buffer. The elution volumes indicated are an average of two independent runs. The column

Interactions between P_{II} and Nitrogenase Regulatory Enzymes

was calibrated with molecular mass markers from Sigma (α -amylase, alcohol dehydrogenase, bovine serum albumin, carbonic anhydrase, and cytochrome *c*). Purified proteins (HisDraT and/or GlnB) were incubated in 50 mM Tris-HCl, pH 8.0, 10% (v/v) glycerol, 100 mM NaCl, 1 mM $MgCl_2$, and 1 mM ADP for 20 min on ice before loading. The loaded samples consisted of GlnB (4 μ mol as trimer), HisDraT (4 μ mol as monomer), or HisDraT plus GlnB (4 μ mol each) in 400 μ l.

Amino Acid Composition—The amino acid composition of the purified DraT-GlnB complex was determined as described (34). To calculate the DraT:GlnB stoichiometry, we used a mathematical model in which we compared the values of the experimental amino acid composition of the complex with the respective amino acid compositions of DraT and GlnB. Asparagine and glutamine are, respectively, converted to aspartate and glutamate; therefore, Asx and Glx correspond to the amount of Asp + Asn and Glu + Gln, because Asn and Gln are deamidated following acid treatment. Norleucine was used as an internal standard, but is not reported.

We used the data from two different estimations of amino acid composition to calculate the stoichiometry (*s*) of the DraT-GlnB complex, with *s* representing the number of GlnB mol for 1 mol of DraT (DraT:*s* GlnB). The value of *s* was calculated using the Solver tool in Microsoft Excel to minimize the mean square deviation between the calculated fractions of each amino acid in the complex and the fractions obtained with the experimental data. The calculated fraction was obtained using Equation 1,

$$\frac{n_{aa}^{DraT-GlnB}}{N^{DraT-GlnB}} = \frac{n_{aa}^{DraT} + (s \times n_{aa}^{GlnB})}{N^{DraT} + (s \times N^{GlnB})} \quad (\text{Eq. 1})$$

where n_{aa} is the number of one particular amino acid in DraT, GlnB, or DraT-GlnB and N is the number of all the amino acids used for the calculation in DraT, GlnB, or DraT-GlnB. All the amino acids reported in supplemental Table S1 were included in the calculation. Valine and isoleucine data were not used, because upon acidic hydrolysis the peptide bonds of Ile-Ile, Val-Val, Ile-Val, and Val-Ile are only partially cleaved, and consequently the values obtained for Val and Ile can be underestimated. DraT and GlnB do not have comparable numbers of those peptide bonds, and, therefore, we did not consider those two residues for estimation of the stoichiometry.

RESULTS

DraG Interaction with GlnZ and GlnZ-UMP₃ in Vitro—We have previously shown that DraG can interact with both uridylylated and de-uridylylated GlnZ *in vivo* and that de-uridylylated GlnZ-DraG interaction is stabilized by ADP. The binary complex contains a 1:1 ratio of GlnZ trimer/DraG monomer (10, 12). To characterize further the effects of GlnZ uridylylation on interaction with DraG, we purified GlnZ and derived GlnZ-UMP₃ by *in vitro* uridylylation (supplemental Fig. S1).

In vitro complex formation between HisDraG and either GlnZ or GlnZ-UMP₃ was assayed by pull-down using Magne-His-Ni²⁺ beads in the presence of ATP, ADP, and 2-OG. Control experiments indicated that neither GlnZ nor GlnZ-UMP₃ bind to the Ni²⁺ beads under the conditions used (data not

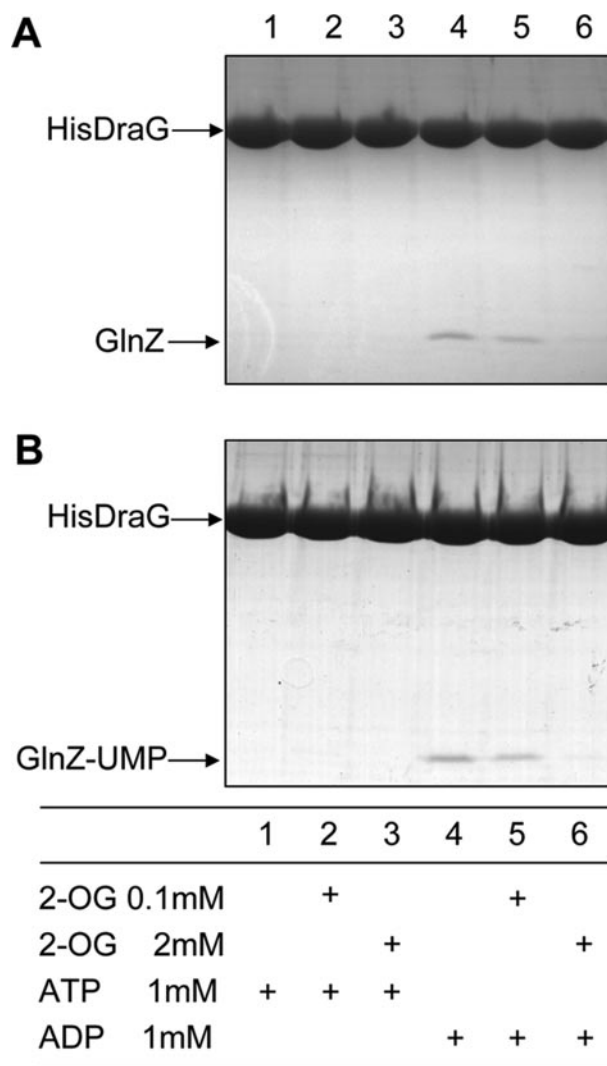


FIGURE 1. *In vitro* formation of the DraG-GlnZ and DraG-GlnZ-UMP₃ complexes. Complex formation was assessed by co-precipitation using Ni²⁺ beads. Reactions were performed in the presence (+) or absence of the effectors (2-OG, ATP, or ADP) as indicated. Binding reactions were conducted in 500 μ l of buffer, adding the purified proteins at concentrations of 0.5 μ M HisDraG and 0.5 μ M GlnZ (A) or GlnZ-UMP₃ (B). The eluted fractions were subjected to SDS-PAGE, the gel was Coomassie Blue-stained. Arrows indicate the identified proteins.

shown). Thus, the presence of GlnZ in the eluate indicates interaction with HisDraG. Both GlnZ and GlnZ-UMP₃ co-purified with HisDraG in the presence of ADP but not in the presence of ATP (Fig. 1) or AMP (data not shown). 2-OG negatively influenced complex formation in the presence of ADP. Fig. 1 shows that the effects of ATP, ADP and 2-OG were not significantly changed whether GlnZ was uridylylated or not (compare Fig. 1, A and B). To determine which form of GlnZ binds preferentially to HisDraG we challenged HisDraG with equimolar amounts of GlnZ and GlnZ-UMP₃ in the presence of ADP. The equimolar GlnZ:GlnZ-UMP ratio was confirmed by analysis on SDS-PAGE (Fig. 2A, lane 1 and supplemental Fig. S2). Quantification of GlnZ after elution of the pull-down assay using HisDraG as bait showed a GlnZ:GlnZ-UMP ratio of \sim 4 (Fig. 2A, lane 2 and supplemental Fig. S2), a result reproduced in two independent experiments. These results, which are in good quantitative agreement with our previous *in vivo* data

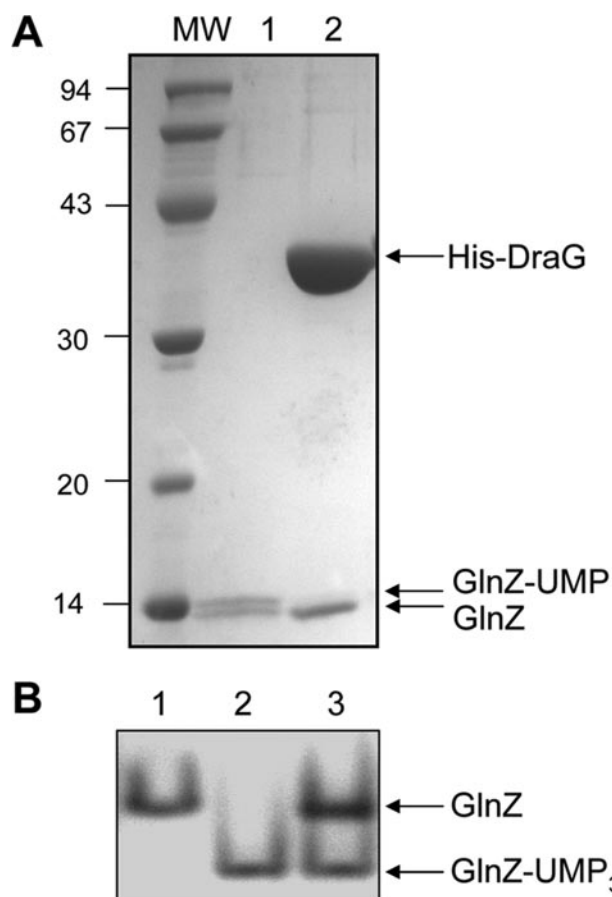


FIGURE 2. Competition assay between GlnZ and GlnZ-UMP₃ to bind DraG. A, complex formation was assessed by co-precipitation using Ni²⁺ beads. Reactions were performed in the presence of ADP. Binding reactions were conducted in 500 μ l of buffer, adding the purified proteins at concentrations of 0.5 μ M HisDraG and 0.5 μ M GlnZ plus GlnZ-UMP₃. The eluted fraction (2) and an equimolar mixture of GlnZ and GlnZ-UMP₃ (1) were subjected to SDS-PAGE and the gel was Coomassie Blue-stained. Arrows indicate the identified proteins. MW indicates molecular weight markers in kDa. B, native-PAGE of GlnZ (1), GlnZ-UMP₃ (2), and an equimolar mixture of GlnZ and GlnZ-UMP₃ (3). The gels were Coomassie Blue-stained.

(10), confirm that DraG can bind to both GlnZ or GlnZ-UMP₃ in the presence of ADP but that the interaction is about four times more favorable when GlnZ is de-uridylylated.

It has been reported that P_{II} proteins from some organisms can form heterotrimers when mixed in solution (35). To confirm that the results reported in Fig. 2A were not caused by the formation of heteromers, *i.e.* GlnZ-UMP₁ or GlnZ-UMP₂, we mixed equimolar amounts of GlnZ and GlnZ-UMP₃, kept these proteins at room temperature for 20 min and then assessed the quaternary structure by native-PAGE. The results in Fig. 2B show that there was no detectable heterotrimer formation under the conditions tested (compare with supplemental Fig. S1B). We did not detect co-purification of either GlnB or GlnB-UMP₃ with HisDraG using ADP in buffers (data not shown). This suggests that DraG cannot interact with GlnB and confirms our previous *in vivo* data (10).

DraT Interaction with GlnB and GlnB-UMP₃ in Vitro—We have previously shown that DraT can interact with de-uridylylated GlnB *in vivo* (10). To characterize the influence of GlnB effectors (ATP, ADP, AMP, and 2-OG) and GlnB uridylylation status on the interaction with DraT we performed pull-down

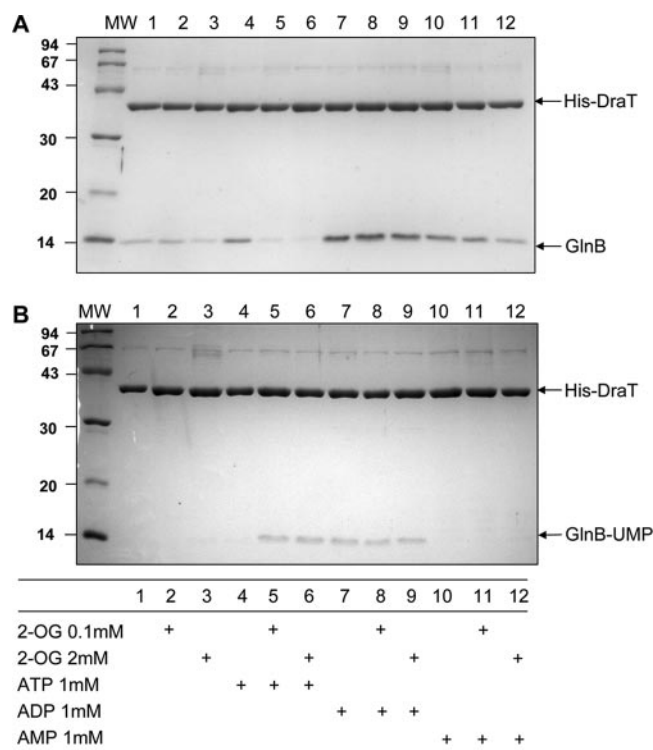


FIGURE 3. *In vitro* formation of the DraT-GlnB and DraT-GlnB-UMP₃ complexes. Complex formation was assessed by co-precipitation using Ni²⁺ beads. Reactions were performed in the presence (+) or absence (-) of the effectors (2-OG, ATP, ADP, and AMP) as indicated. Binding reactions were conducted in 500 μ l of buffer, adding the purified proteins at concentrations of 0.5 μ M HisDraT and 0.5 μ M GlnB (A) or GlnB-UMP₃ (B). The eluted fractions were subjected to SDS-PAGE, and the gels were Coomassie Blue-stained. Arrows indicate the identified proteins.

assays where HisDraT was immobilized on nickel beads and challenged with either GlnB or GlnB-UMP₃. Negative controls indicate that neither GlnB nor GlnB-UMP₃ bind to the beads under the conditions used (data not shown).

GlnB co-purified with HisDraT in all conditions tested although there were substantial differences in the amount of GlnB recovered with HisDraT according to the presence of nucleotides and/or 2-OG in the buffers (Fig. 3A and supplemental Fig. S3A). The GlnB signal in the eluate was stronger when ADP was present (Fig. 3A; lanes 7, 8, and 9) and addition of 2-OG did not alter the capacity of GlnB to interact with HisDraT. However, when ATP was used alone the GlnB signal in the eluate decreased 2-fold when compared with ADP (compare Fig. 3A, lanes 4 and 7). The combination of ATP and 2-OG almost abolished complex formation (Fig. 3A, lanes 5 and 6). AMP was also capable of stimulating complex formation (Fig. 3A, compare lanes 1 and 10) and the AMP-stimulating effect was slightly counteracted by the presence of 2-OG (Fig. 3A, compare lanes 10 and 12). When the experiment in Fig. 3A was performed in the presence of the DraT substrate, NAD⁺ 1 mM, similar results were obtained (data not shown).

To confirm the negative effects of ATP in combination with 2-OG on HisDraT-GlnB complex formation we immobilized the complex on Ni²⁺ beads in the presence of ADP and then subjected the sample to a wash step in buffer containing ADP, ADP plus 2-OG, ATP, or ATP plus 2-OG. The results (Fig. 4) confirmed that the DraT-GlnB complex is destabilized in the

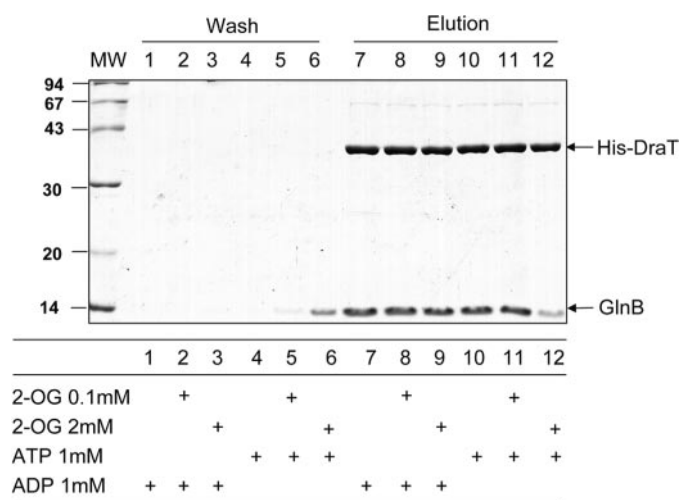


FIGURE 4. The presence of 2-OG and ATP destabilizes the DraT-GlnB complex. A, HisDraT-GlnB complex was immobilized on Ni^{2+} beads in buffer containing 1 mM ADP. Beads were washed (*Wash*) with buffer containing ADP or ATP and 2-OG as indicated. Bound proteins were eluted in SDS-PAGE sample buffer (*Elution*). The samples were applied to SDS-PAGE, and the gels were stained with Coomassie Blue. Arrows indicate the identified proteins. MW, molecular weight markers in kDa.

presence of a combination of ATP and 2-OG and that dissociation of the complex is further enhanced by a high concentration of 2-OG.

We also evaluated the effects of different combinations of ADP and ATP on HisDraT-GlnB complex formation, under low (0.1 mM) or high (2 mM) concentrations of 2-OG. ATP inhibited complex formation in a 2-OG concentration-dependent manner despite the presence of ADP in the buffers (Fig. S4), indicating that ATP and ADP compete for the nucleotide-binding sites of GlnB.

Unexpectedly, when we challenged immobilized HisDraT to bind GlnB-UMP₃ we observed a different response in comparison to results obtained with de-uridylylated GlnB (compare Fig. 3, A and B and supplemental Fig. S3, A and B). We did not detect interactions between HisDraT and GlnB-UMP₃ in the absence of nucleotides or in the presence of AMP (Fig. 3B, lanes 1–3 and 10–12). A considerably different pattern of complex formation in response to ATP was observed depending on whether GlnB was uridylylated or not (compare Fig. 3, A and B, lanes 4–6). ATP-stimulated complex formation with de-uridylylated GlnB but not with GlnB-UMP₃. Furthermore, when ATP and 2-OG were combined there was inhibition of complex formation between HisDraT and GlnB but there was stimulation of complex formation between HisDraT and GlnB-UMP₃. The only common pattern that emerge from Fig. 3, A (GlnB) and B (GlnB-UMP₃) is the stimulatory effect of ADP on complex formation regardless of the presence of 2-OG.

Together, the results shown in Fig. 3 suggest that optimum conditions for DraT-GlnB complex formation require de-uridylylated GlnB and high ADP. To assess the relative binding affinity of GlnB, GlnZ, GlnB-UMP₃, and GlnZ-UMP₃ toward HisDraT we challenged HisDraT with all four P_{II} proteins in the presence of ADP. The results (supplemental Fig. S5) indicate that HisDraT does not interact with GlnZ under the conditions tested and that, although both GlnB and GlnB-UMP₃ can inter-

act with HisDraT, the amount of de-uridylylated GlnB recovered was 3-fold higher than GlnB-UMP₃. We were not able to perform internal competition experiments between GlnB and GlnB-UMP₃, as reported for the HisDraG-GlnZ interaction (Fig. 2A), because the poor separation between GlnB and GlnB-UMP monomers on SDS-PAGE did not allow accurate signal quantification.

Gel Filtration of the DraT-GlnB Complex—In our pull-down assays, the DraT-GlnB complex was very stable in the presence of ADP (Fig. 3), and consequently to determine the stoichiometry of the complex, we performed gel filtration of the proteins alone or together with ADP in the buffer. GlnB eluted from the gel filtration column as a single peak at 12.49 ± 0.08 ml (supplemental Fig. S6A), corresponding to an apparent molecular mass of 29 kDa, which is similar to that predicted for the GlnB trimer (36 kDa).

HisDraT alone did not give any clear peak on the gel filtration column as monitored by the UV absorption profile. Eluted samples were analyzed by SDS-PAGE and gave a very faint signal for HisDraT (supplemental Fig. S6B), with no signal in the void volume. Analysis of the eluted samples by Western blot using anti-DraT antibody confirmed that HisDraT eluted as a broad peak between 12 and 15 ml, peaking at 13.5 ml (supplemental Fig. S6C). This corresponds to a range of molecular mass from 5 to 40 kDa. Hence as HisDraT, which has a predicted molecular mass of 35 kDa, eluted as a smear we assumed that HisDraT is somehow interacting with the column matrix. However when we loaded a mixture of DraT and GlnB in a 1:1 molar ratio (monomer to trimer, respectively) all the protein eluted in a single peak (11.36 ± 0.05 ml), corresponding to ~ 64 kDa (Fig. 5). The apparent change in the interaction of HisDraT with the column matrix when GlnB was also present suggests that HisDraT might undergo a conformational change upon complex formation with GlnB.

GlnB May Induce a Conformational Change in DraT upon Complex Formation—In the pull-down experiments with HisDraT and GlnB, we observed that the amount of HisDraT eluted from the Ni^{2+} beads using imidazole depended on the conditions (*i.e.* the presence of ATP, ADP, or 2-OG) and that there was a clear correlation between the amount of GlnB in the eluate (indicative of complex formation) and the amount of HisDraT eluted with imidazole. This GlnB dependence is exemplified in Fig. 6. In all lanes, the same amount of HisDraT was added to the Ni^{2+} beads. GlnB was also added for lanes 1–3, and pull-down experiments were performed in the presence of ADP and 2-OG as indicated in the figure. When the proteins were eluted with 500 mM imidazole (Fig. 6A), about 30% more HisDraT was recovered in the eluate when GlnB was present. Such a difference was not observed under conditions where GlnB did not interact with HisDraT, *i.e.* in the presence of ATP and high 2-OG (data not shown). To check if proteins were still bound to the resin after addition of imidazole, the beads were further treated with SDS-PAGE sample buffer and this second elution step was loaded on another gel (Fig. 6B). Quantification of the protein bands indicated that 50% less HisDraT remained bound to the beads in the presence of GlnB (Fig. 6B). The alteration in the apparent affinity of HisDraT for the Ni^{2+} beads upon complex formation with GlnB suggests that complex formation results in a conforma-

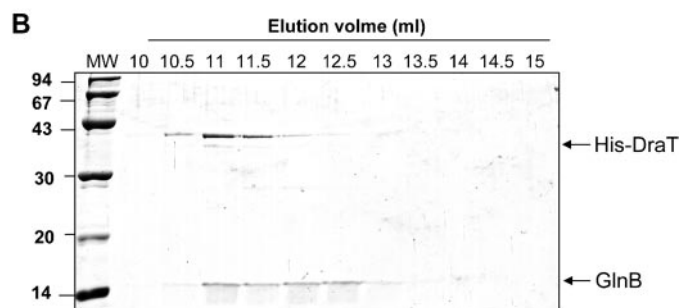
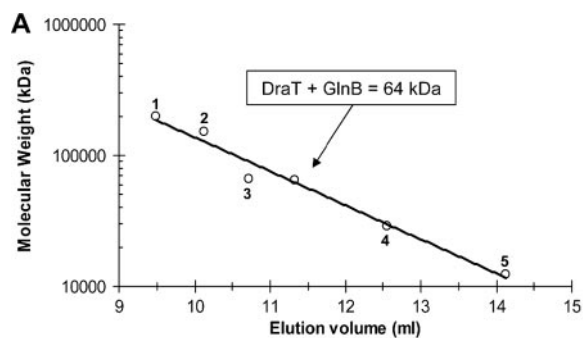


FIGURE 5. Gel filtration analysis of the DraT-GlnB complex. Gel filtration was performed on a Superose 12 10/30 GL column using 50 mM Tris-HCl, pH 8.0, 10% (v/v) glycerol, 0.05% (w/v) Tween 20, 100 mM NaCl, 1 mM MgCl₂, 1 mM ADP as buffer. Runs were performed at room temperature at a flow rate of 0.5 ml·min⁻¹, and the column was calibrated with a range of molecular mass standards (Sigma). Purified proteins (HisDraT and GlnB) were incubated in 50 mM Tris-HCl, pH 8.0, 10% (v/v) glycerol, 0.05% (w/v) Tween 20, 100 mM NaCl, 1 mM MgCl₂, and 1 mM ADP for 20 min on ice before loading. **A**, elution volume of the DraT-GlnB complex (11.36 ml; 64 kDa) and of the Sigma molecular weight calibrants 1 to 5 (1, α -amylase, 200 kDa, 9.49 ml; 2, alcohol dehydrogenase, 150 kDa, 10.13 ml; 3, bovine serum albumin, 66 kDa, 10.72 ml; 4, carbonic anhydrase, 29 kDa, 12.55 ml; 5, cytochrome c, 12.4 kDa, 14.13 ml. **B**, when HisDraT plus GlnB were loaded, aliquots of 500 μ l were collected, and 10 μ l were analyzed on 12.5% SDS-PAGE gels. Arrows indicate the identified proteins. MW, molecular weight markers in kDa.

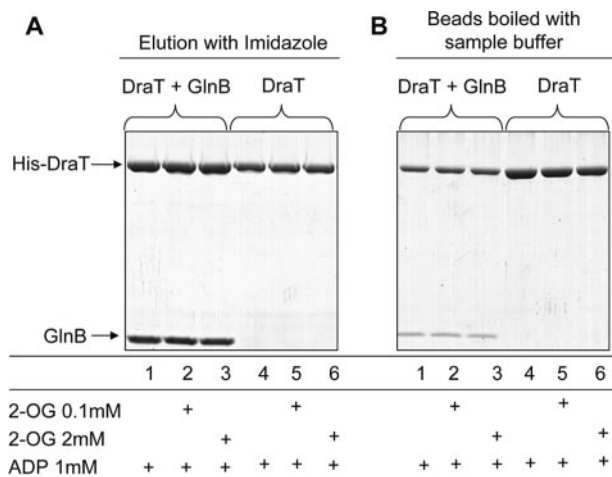


FIGURE 6. HisDraT has lower affinity for Ni²⁺ when complexed with GlnB. The HisDraT-GlnB complex (lanes 1–3) or HisDraT alone (lanes 4–6) were immobilized on Ni²⁺ beads in binding buffer containing 1 mM ADP and 2-OG as indicated. After extensive washing, bound proteins were eluted with 0.5 M imidazole (**A**). The proteins that remained bound to the beads were further eluted by boiling the beads in SDS-PAGE sample buffer for 5 min (**B**). The samples were applied to SDS-PAGE, and the gels were stained with Coomassie Blue. Arrows indicate the identified proteins.

tional change of DraT. Alternatively, this phenomenon could be explained by a simple occlusion of the His-Tag of DraT due to steric effects upon complex formation.

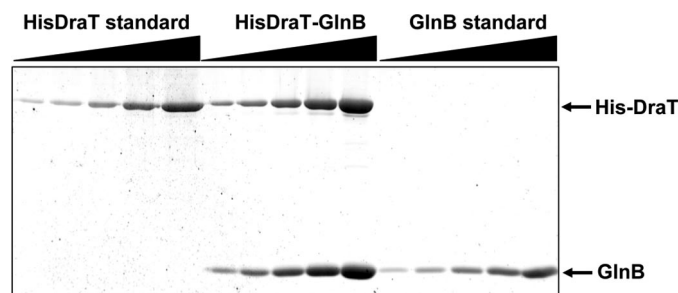


FIGURE 7. The purified DraT-GlnB complex shows a monomer to trimer stoichiometry. Purified HisDraT and GlnB were used as standards to determine the molar concentration of both HisDraT and GlnB in the purified DraT-GlnB complex as described under "Experimental Procedures." Proteins were analyzed on 12.5% SDS-PAGE gels stained with SYPRO-Ruby.

Purification of the DraT-GlnB Complex—Expression of HisDraT in *E. coli* BL21 showed that the protein is predominantly found in insoluble inclusion bodies after cell disruption, this occurs even when the induction is performed at low temperature (supplemental Fig. S7A). Interestingly, we observed that co-expression with GlnB promotes a significant solubilization of HisDraT, which again suggests a possible conformational change in DraT upon GlnB binding. As the DraT-GlnB complex is more stable in ADP we carried out the purification of the complex using a HiTrap chelating Ni²⁺ column with 0.5 mM ADP in all buffers. After the Ni²⁺ column, two major bands were observed in SDS-PAGE ~37 kDa and ~13 kDa (supplemental Fig. S7B). These bands were assigned as *A. brasilense* DraT (37% coverage) and GlnB (75% coverage), respectively, after trypsin digestion and MALDI-TOF peptide mass fingerprint analysis using Mascot 2.2. We also used whole protein MALDI-TOF analysis to determine the uridylylation status of GlnB that co-purifies with HisDraT, this analysis yielded a single peak with m/z ratio of 12,367, which is in good agreement with the predicted monomeric molecular mass of non-uridylylated GlnB (12, 37).

Stoichiometry of the Purified DraT-GlnB Complex—We investigated the stoichiometry of the purified complex by quantitative SDS-PAGE stained with SYPRO-Ruby (Fig. 7). For this, known amounts of GlnB and HisDraT were loaded in a gel alongside several dilutions of the purified complex. The standard curves for both GlnB and HisDraT were linear with an R^2 of 0.991 and 0.999, respectively. Three lanes of the complex dilutions that fell within the linear region of the standard curves were used to determine the stoichiometry of the complex as $1:0.86 \pm 0.14$ (molar ratio of DraT monomer:GlnB trimer). Moreover, as the molecular mass of HisDraT (37,342 Da) is similar to that of the GlnB trimer (37,113 Da) we expected an almost equal intensity for the SYPRO-Ruby signals of HisDraT and GlnB for a complex containing 1 DraT monomer and 1 GlnB trimer. Indeed, the HisDraT:GlnB signal ratio was $1:0.9 \pm 0.08$ (calculated from the five lanes in Fig. 7), which agrees with the proposed stoichiometry.

We also performed an amino acid composition analysis of the purified DraT-GlnB complex, using duplicate samples (supplemental Table S1). The stoichiometry calculated using these data were 1:1.15 (DraT monomer:GlnB trimer), in close agreement with the gel densitometric analysis.

DISCUSSION

In Vitro Complex Formation between DraT and GlnB—We have previously shown that *A. brasilense* DraT interacts with GlnB *in vivo*, after an ammonium shock; conditions where DraT should be active (10). Using a yeast two-hybrid system, DraT has also been shown to interact with GlnB in *R. rubrum* (36) and *R. capsulatus* (37). We have now shown, for the first time, that DraT and GlnB can form a complex *in vitro* (Fig. 3). All adenine nucleotides tested (AMP, ADP, and ATP) stimulated DraT-GlnB complex formation and 2-OG inhibited complex formation when ATP or AMP, but not ADP, were present (Fig. 3). The HisDraT-GlnB complex could be co-purified from *E. coli* in the presence of ADP (supplemental Fig. S7B). These results suggest that DraT-GlnB complex formation responds to the intracellular energy charge as well as the 2-OG concentration. Although we cannot exclude that the P_{II} effectors can bind to DraT, we believe that these molecules alter DraT-GlnB complex stability by changing the structure of the GlnB trimer. To our knowledge, this is the first report suggesting that AMP can also be sensed by a P_{II} protein, and hence the intracellular concentration of AMP might also influence P_{II} protein activity.

Interestingly we found that GlnB-UMP₃ can also interact with DraT under some conditions. The response to P_{II} protein effectors was very different from that observed with de-uridylylated GlnB, the only common feature of DraT-GlnB and DraT-GlnB-UMP₃ complex formation being the stimulatory effect of ADP. By comparison the response of the DraG-GlnZ complex to effectors was unaffected by the uridylylation status of GlnZ (Fig. 1). We did not expect to see interaction between DraT and GlnB-UMP₃ *in vitro* since we did not detect it *in vivo* (10). However in our *in vivo* experiments there was no ADP in the washing buffers to stabilize a DraT-GlnB-UMP₃ complex. This, together with the relatively low affinity binding between DraT and GlnB-UMP₃ (supplemental Fig. S5), might have resulted in loss of GlnB-UMP₃ from the complex during the *in vivo* assay.

Based on our previous *in vivo* data, we proposed that the DraT recognition by GlnB involves the T-loop region of GlnB, while conversely the DraG recognition surface of GlnZ does not involve the T-loops, the sites where the uridylylation occurs (10). This hypothesis agrees with the experimental data, in that the uridylylation status of GlnB plays an important role in the pattern of DraT-GlnB complex formation in response to the P_{II} effectors (Fig. 3) whereas the response of DraG-GlnZ complex formation to P_{II} effectors was unaffected by the uridylylation state of GlnZ (Fig. 1). Furthermore, mutagenesis of *R. rubrum* GlnB and yeast two-hybrid analysis of the *R. rubrum* DraT-GlnB complex also suggests that the GlnB T-loop is involved in the interaction with DraT (37).

Intriguingly the DraT-GlnB complex formation response to ATP was dependent on the uridylylation state of GlnB (Fig. 3). While ATP alone stimulated complex formation with de-uridylylated GlnB, it did not with GlnB-UMP₃. Furthermore, a combination of ATP and 2-OG inhibited complex formation between HisDraT and GlnB but stimulated complex formation with GlnB-UMP₃. Assuming that neither ATP nor 2-OG can bind DraT, then the stimulatory effect of 2-OG in combination

with ATP on DraT-GlnB-UMP₃ complex formation suggests that GlnB-UMP₃ can also bind 2-OG, a feature already reported for *E. coli* GlnB (38).

Stoichiometry of the DraT-GlnB Complex and Evidence for Conformational Changes in DraT upon Complex Formation—Gel filtration analysis, quantitative SDS-PAGE, and amino acid composition analysis of the DraT-GlnB complex all indicated a stoichiometry of 1:1, DraT monomer to GlnB trimer. Other P_{II} complexes have been reported with this stoichiometry, *i.e.* one target monomer to one P_{II} trimer, including *A. brasilense* DraG-GlnZ (12), *Synechococcus* sp. PipX- P_{II} (39), and *E. coli* ATase-GlnB (40). This raises interesting questions about the likely structure of such complexes because in the structures of P_{II} complexes determined so far, the P_{II} target protein is either trimeric or hexameric and exhibits 3-fold symmetry (27, 41, 42).

Gel filtration analysis of DraT with GlnB, together with the observed influence of GlnB on altering both the solubility and the affinity of HisDraT for binding Ni²⁺ upon complex formation, support the proposal for conformational changes in DraT upon complex formation with GlnB. The DraT enzyme was previously purified to near homogeneity from *R. rubrum* (43). DraT activity was only stable when ADP was present in the purification buffers, and the purified fractions of DraT analyzed on SDS-PAGE indicated the presence of a contaminant band with an apparent molecular weight close to that expected for a P_{II} protein monomer (43). The identity of this band is not known, but the authors noted that attempts to remove this contaminant resulted in loss of DraT activity. All of the above observations are consistent with our data. Hence it is possible that the activity of the partially purified *R. rubrum* DraT preparation was due to the presence of a P_{II} protein. Furthermore it was also observed that *R. rubrum* DraT activity was more stable if ammonia-grown cells were used as the source of the enzyme (43). Under these conditions, GlnB should be completely de-uridylylated and should form a tight complex with DraT in the presence of ADP (Fig. 3A) thereby effecting DraT activation by conformational change.

Putative Physiological Relevance of the P_{II} Effectors on Nitrogenase Switch-off—Both the DraG-GlnZ and DraT-GlnB complexes respond to the intracellular energy charge (ATP/ADP ratio), to the 2-OG concentration and to the intracellular nitrogen status (glutamine levels) as signaled by the uridylylation status of GlnZ and GlnB. Both complexes were more stable in the presence of ADP, low 2-OG concentrations, and when P_{II} proteins were de-uridylylated. It has been shown in *E. coli* and in other organisms that when ammonium-limited cells are subjected to an ammonium shock, there are transitory fluctuations in the intracellular glutamine, 2-OG and ATP levels (44–46). Based on these observations we now propose a model to address the physiological relevance of the P_{II} effectors on nitrogenase switch-off (Fig. 8).

Under nitrogen-fixing conditions (Fig. 8A) the intracellular glutamine levels are low and 2-OG accumulates. The ATP/ADP ratio must be high to support nitrogenase activity. GlnB and GlnZ are fully uridylylated and presumably bound to ATP and 2-OG which results in loose, if any, association with DraT and DraG, respectively. DraG is catalytically active and DraT is not, thus NifH is not modified allowing

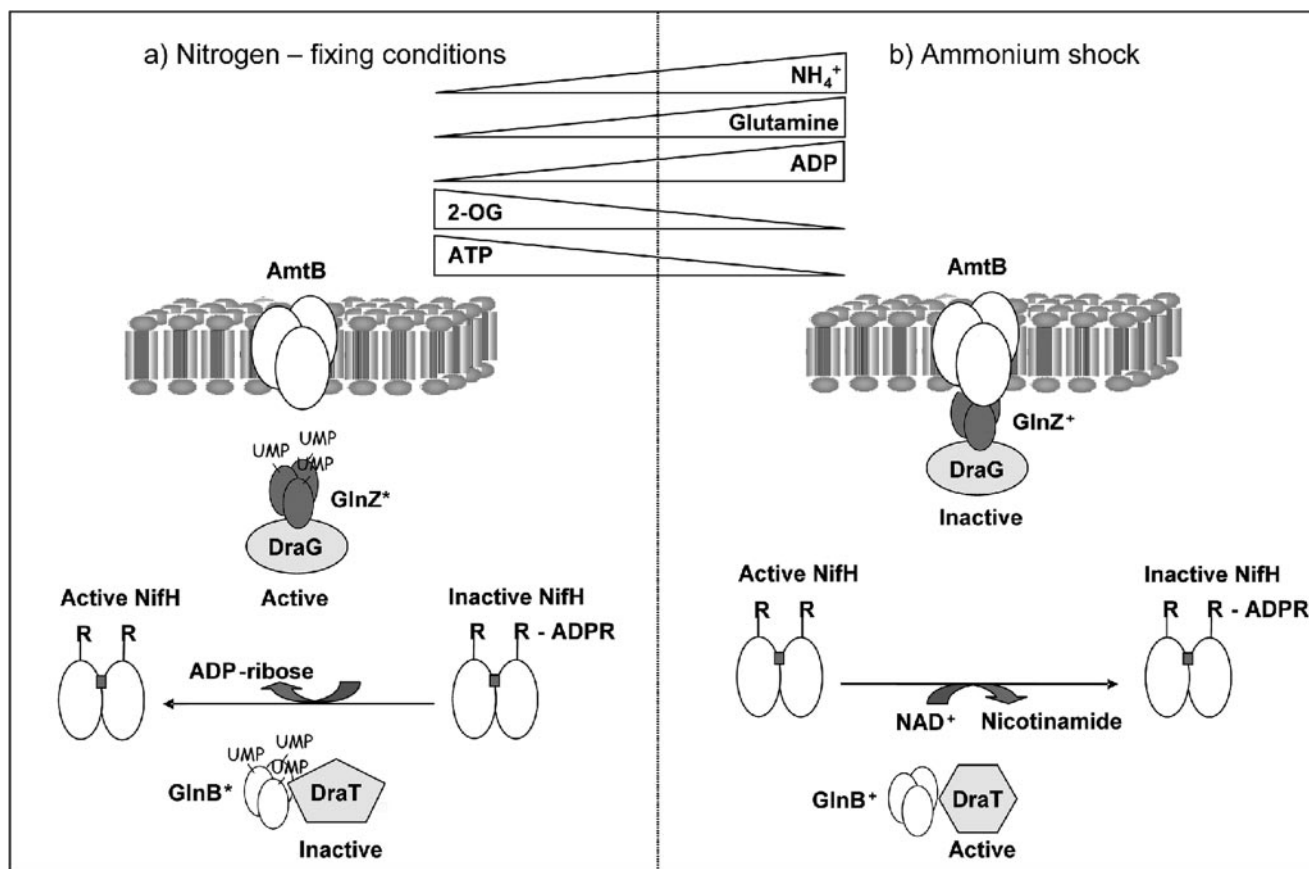


FIGURE 8. Model for the role of P_{II} protein effectors in the regulation of DraT and DraG activities in response to ammonium in *A. brasilense*. $GlnB^+$ and $GlnZ^+$ indicate fully uridylylated proteins bound to ATP and 2-OG. $GlnB^*$ and $GlnZ^*$ indicate de-uridylylated proteins bound to ADP.

full nitrogenase activity. Following an ammonium shock (Fig. 8B) the intracellular glutamine concentration increases triggering GlnD-mediated de-uridylylation of GlnB and GlnZ (30, 31) and reciprocally the intracellular 2-OG concentration falls. Ammonium flux through GS should also reduce the ATP/ADP ratio. De-uridylylated GlnB and GlnZ are presumably, in an ADP-bound form which results in formation of DraT-GlnB, DraG-GlnZ, and AmtB-GlnZ complexes. This process efficiently targets DraG to the cell membrane through the formation of a ternary complex involving AmtB, GlnZ, and DraG, which inactivates the enzyme (12). Binding of de-uridylylated GlnB to DraT results in conformational change and activation of DraT with resultant NifH modification and nitrogenase switch-off.

Another possible outcome of the high flux of glutamine through GOGAT after an ammonium shock is a sudden increase in intracellular $NADP^+$. $NADP^+$ has been shown to act as a substrate of *R. rubrum* DraT (47), and increased levels of $NADP^+$ might further increase DraT activity. DraT has been shown to be more active *in vitro* toward NifH bound to MgADP, whereas DraG is more active when NifH is bound to MgATP (43, 48). Hence, a decrease in the ATP/ADP ratio after an ammonium shock could promote inactivation of nitrogenase by DraT. Moreover, the ATP/ADP ratio also regulates nitrogenase activity *in vitro* (5), not only because the enzyme requires substitution of ADP bound to NifH by ATP during the electron transfer catalytic cycle (49) but also because the ADP-

bound NifH competes with ATP-bound NifH for binding to MoFe-protein (50). Consequently a decrease in cellular energy charge might facilitate another level of regulation of nitrogenase activity, independent of NifH modification.

This multi-tier regulatory cascade would provide very fine tuning of nitrogenase activity depending on the energy charge (ATP/ADP ratio), carbon status (2-OG levels), and nitrogen status (sensed through the P_{II} modification status and through the downstream metabolic effects of ammonium assimilation). Such a system would not only minimize the waste of metabolic energy to fix nitrogen when ammonium is present in the environment but would also coordinate ammonium production and assimilation with carbon and energy metabolism. This intricate regulation of nitrogenase could confer a considerable metabolic advantage in very competitive niches such as the soil and rhizosphere where *A. brasilense* is commonly found.

Acknowledgments—We thank Maria Carolina C. Huergo for helping with the figures and Fábio C. Gozzo (Laboratório Nacional de Luz Síncrotron) for allowing our access to the Mascot server at the LNLs. Amino acid composition analysis was carried out by Peter Sharatt (Protein and Nucleic Acid Chemistry Facility, Dept. of Biochemistry, University of Cambridge). We are grateful to Stephen Bornemann (John Innes Centre) for advice regarding stoichiometry determination from amino acid composition. Valter de Baura, Roseli Prado, and Julieta Pie are thanked for their technical support.

REFERENCES

- Dixon, R., and Kahn, D. (2004) *Nat. Rev. Microbiol.* **2**, 621–631
- Nordlund, S. (2000) in *Prokaryotic Nitrogen Fixation: A Model System for Analysis of Biological Processes* (Triplett, E. W., ed) pp. 149–167, Horizon Scientific Press, Wymondham, UK
- Zhang, Y., Burris, R. H., Ludden, P. W., and Roberts, G. P. (1997) *FEMS Microbiol. Lett.* **152**, 195–204
- Chapman, A. G., Fall, L., and Atkinson, D. E. (1971) *J. Bacteriol.* **108**, 1072–1086
- Upchurch, R. G., and Mortenson, L. E. (1980) *J. Bacteriol.* **143**, 274–284
- Tremblay, P. L., Drepper, T., Masepohl, B., and Hallenbeck, P. C. (2007) *J. Bacteriol.* **189**, 5850–5859
- Tremblay, P. L., and Hallenbeck, P. C. (2008) *J. Bacteriol.* **190**, 1588–1594
- Zhang, Y., Wolfe, D. M., Pohlmann, E. L., Conrad, M. C., and Roberts, G. P. (2006) *Microbiology* **152**, 2075–2089
- Wang, H., Franke, C. C., Nordlund, S., and Noren, A. (2005) *FEMS Microbiol. Lett.* **253**, 273–279
- Huergo, L. F., Chubatsu, L. S., Souza, E. M., Pedrosa, F. O., Steffens, M. B., and Merrick, M. (2006) *FEBS Lett.* **580**, 5232–5236
- Huergo, L. F., Souza, E. M., Araujo, M. S., Pedrosa, F. O., Chubatsu, L. S., Steffens, M. B., and Merrick, M. (2006) *Mol. Microbiol.* **59**, 326–337
- Huergo, L. F., Merrick, M., Pedrosa, F. O., Chubatsu, L. S., Araujo, L. M., and Souza, E. M. (2007) *Mol. Microbiol.* **66**, 1523–1535
- de Zamaroczy, M. (1998) *Mol. Microbiol.* **29**, 449–463
- Forchhammer, K. (2008) *Trends Microbiol.* **16**, 65–77
- Leigh, J. A., and Dodsworth, J. A. (2007) *Annu. Rev. Microbiol.* **61**, 349–377
- Carr, P. D., Cheah, E., Suffolk, P. M., Vasudevan, S. G., Dixon, N. E., and Ollis, D. L. (1996) *Acta Crystallogr.* **D52**, 93–104
- Xu, Y., Cheah, E., Carr, P. D., van Heeswijk, W. C., Westerhoff, H. V., Vasudevan, S. G., and Ollis, D. L. (1998) *J. Mol. Biol.* **282**, 149–165
- Atkinson, M. R., Kamberov, E. S., Weiss, R. L., and Ninfa, A. J. (1994) *J. Biol. Chem.* **269**, 28288–28293
- Strosser, J., Ludke, A., Schaffer, S., Kramer, R., and Burkovski, A. (2004) *Mol. Microbiol.* **54**, 132–147
- Forchhammer, K. (2004) *FEMS Microbiol. Rev.* **28**, 319–333
- Kamberov, E. S., Atkinson, M. R., and Ninfa, A. J. (1995) *J. Biol. Chem.* **270**, 17797–17807
- Xu, Y., Carr, P. D., Huber, T., Vasudevan, S. G., and Ollis, D. L. (2001) *Eur. J. Biochem.* **268**, 2028–2037
- Yildiz, O., Kalthoff, C., Raunser, S., and Kuhlbrandt, W. (2007) *EMBO J.* **26**, 589–599
- Jiang, P., and Ninfa, A. J. (2007) *Biochemistry* **46**, 12979–12996
- Wolfe, D. M., Zhang, Y., and Roberts, G. P. (2007) *J. Bacteriol.* **189**, 6861–6869
- Teixeira, P. F., Jonsson, A., Frank, M., Wang, H., and Nordlund, S. (2008) *Microbiology* **154**, 2336–2347
- Conroy, M. J., Durand, A., Lupo, D., Li, X. D., Bullough, P. A., Winkler, F. K., and Merrick, M. (2007) *Proc. Natl. Acad. Sci. U. S. A.* **104**, 1213–1218
- de Zamaroczy, M., Paquelin, A., Peltre, G., Forchhammer, K., and Elmerich, C. (1996) *J. Bacteriol.* **178**, 4143–4149
- van Dommelen, A., Keijers, V., Somers, E., and Vanderleyden, J. (2002) *Mol. Genet. Genomics* **266**, 813–820
- Araujo, L. M., Huergo, L. F., Invitti, A. L., Gimenes, C. I., Bonatto, A. C., Monteiro, R. A., Souza, E. M., Pedrosa, F. O., and Chubatsu, L. S. (2008) *Braz. J. Med. Biol. Res.* **41**, 289–294
- Araujo, M. S., Baura, V. A., Souza, E. M., Benelli, E. M., Rigo, L. U., Steffens, M. B., Pedrosa, F. O., and Chubatsu, L. S. (2004) *Protein Expr. Purif.* **33**, 19–24
- Huergo, L. F., Souza, E. M., Steffens, M. B., Yates, M. G., Pedrosa, F. O., and Chubatsu, L. S. (2005) *Arch. Microbiol.* **183**, 209–217
- Huergo, L. F., Filipaki, A., Chubatsu, L. S., Yates, M. G., Steffens, M. B., Pedrosa, F. O., and Souza, E. M. (2005) *FEMS Microbiol. Lett.* **253**, 47–54
- Durand, M., and Merrick, M. (2006) *J. Biol. Chem.* **281**, 29558–29567
- Forchhammer, K., Hedler, A., Strobel, H., and Weiss, V. (1999) *Mol. Microbiol.* **33**, 338–349
- Zhu, Y., Conrad, M. C., Zhang, Y., and Roberts, G. P. (2006) *J. Bacteriol.* **188**, 1866–1874
- Pawlowski, A., Riedel, K. U., Klipp, W., Dreiskemper, P., Gross, S., Bierhoff, H., Drepper, T., and Masepohl, B. (2003) *J. Bacteriol.* **185**, 5240–5247
- Jiang, P., Peliska, J. A., and Ninfa, A. J. (1998) *Biochemistry* **37**, 12782–12794
- Espinosa, J., Forchhammer, K., Burillo, S., and Contreras, A. (2006) *Mol. Microbiol.* **61**, 457–469
- Jiang, P., Pioszak, A. A., and Ninfa, A. J. (2007) *Biochemistry* **46**, 4117–4132
- Llacer, J. L., Contreras, A., Forchhammer, K., Marco-Marin, C., Gil-Ortiz, F., Maldonado, R., Fita, I., and Rubio, V. (2007) *Proc. Natl. Acad. Sci. U. S. A.* **104**, 17644–17649
- Mizuno, Y., Moorhead, G. B. G., and Ng, K. K. (2007) *J. Biol. Chem.* **282**, 35733–35740
- Lowery, R. G., and Ludden, P. W. (1988) *J. Biol. Chem.* **263**, 16714–16719
- Senior, P. J. (1975) *J. Bacteriol.* **123**, 407
- Paul, T. D., and Ludden, P. W. (1984) *Biochem. J.* **224**, 961–969
- Li, J., Hu, C.-Z., and Yoch, D. C. (1987) *J. Bacteriol.* **169**, 231–237
- Ponnuraj, R. K., Rubio, L. M., Grunwald, S. K., and Ludden, P. W. (2005) *FEBS Lett.* **579**, 5751–5758
- Saari, L. L., Triplett, E. W., and Ludden, P. W. (1984) *J. Biol. Chem.* **259**, 15502–15508
- Burris, R. H. (1991) *J. Biol. Chem.* **266**, 9339–9342
- Tezcan, F. A., Kaiser, J. T., Mustafi, D., Walton, M. Y., Howard, J. B., and Rees, D. C. (2005) *Science* **309**, 1377–1380